

Hypothesis Paper

Martian CH₄: Sources, Flux, and Detection

T.C. ONSTOTT,^{1,2} D. MCGOWN,^{1,2} J. KESSLER,^{1,2} B. SHERWOOD LOLLAR,^{2,3}
K.K. LEHMANN,^{2,4} and S.M. CLIFFORD^{2,5}

ABSTRACT

Recent observations have detected trace amounts of CH₄ heterogeneously distributed in the martian atmosphere, which indicated a subsurface CH₄ flux of $\sim 2 \times 10^5$ to 2×10^9 cm⁻² s⁻¹. Four different origins for this CH₄ were considered: (1) volcanogenic; (2) sublimation of hydrate-rich ice; (3) diffusive transport through hydrate-saturated cryosphere; and (4) microbial CH₄ generation above the cryosphere. A diffusive flux model of the martian crust for He, H₂, and CH₄ was developed based upon measurements of deep fracture water samples from South Africa. This model distinguishes between abiogenic and microbial CH₄ sources based upon their isotopic composition, and couples microbial CH₄ production to H₂ generation by H₂O radiolysis. For a He flux of $\sim 10^5$ cm⁻² s⁻¹ this model yields an abiogenic CH₄ flux and a microbial CH₄ flux of $\sim 10^6$ and $\sim 10^9$ cm⁻² s⁻¹, respectively. This flux will only reach the martian surface if CH₄ hydrate is saturated in the cryosphere; otherwise it will be captured within the cryosphere. The sublimation of a hydrate-rich cryosphere could generate the observed CH₄ flux, whereas microbial CH₄ production in a hypersaline environment above the hydrate stability zone only seems capable of supplying $\sim 10^5$ cm⁻² s⁻¹ of CH₄. The model predicts that He/H₂/CH₄/C₂H₆ abundances and the C and H isotopic values of CH₄ and the C isotopic composition of C₂H₆ could reveal the different sources. Cavity ring-down spectrometers represent the instrument type that would be most capable of performing the C and H measurements of CH₄ on near future rover missions and pinpointing the cause and source of the CH₄ emissions. **Key Words:** Mars—Methane—Methanogens—Fischer-Tropsch reactions—Infrared spectroscopy. *Astrobiology* 6, 377–395.

INTRODUCTION

THE RECENT DETECTION of at least ~ 10 parts per billion (ppbv) CH₄ in the martian atmosphere has fueled speculation that CH₄ may originate by microbial methanogenesis in the regolith of Mars

(Formisano *et al.*, 2004; Krasnopolsky *et al.*, 2004a,b; Mumma *et al.*, 2004). This is because the rate of photochemical destruction of CH₄ is approximately 2.2×10^5 cm⁻² s⁻¹ (1.7×10^7 mol year⁻¹), which translates into a CH₄ lifetime of ~ 340 years for ~ 10 ppbv (Krasnopolsky *et al.*,

Departments of ¹Geosciences and ⁴Chemistry, Princeton University, Princeton, New Jersey.

²Indiana Princeton Tennessee Astrobiology Initiative (IPTAI), NASA Astrobiology Institute, Indiana University, Bloomington, Indiana.

³Department of Geology, University of Toronto, Toronto, Ontario, Canada.

⁵Lunar Planetary Institute, Houston, Texas.

2004b). The short lifetime implies an active CH₄ source such as autotrophic methanogenesis (4H₂ + CO₂ → CH₄ + 2H₂O) combined with diffusion through the regolith (where production occurs in near-surface brines) or through the underlying cryosphere (where production occurs in a subpermafrost aquifer), the sublimation or depressurization of hydrate-rich ground ice (Max and Clifford, 2000), or recent CH₄-generating events such as cometary impact (Kress and McKay, 2004), igneous intrusion (Lyons *et al.*, 2005), volcanic eruption, or thermally generated gas discharge (Wong and Atreya, 2003). The last three mechanisms appear not to be supported by spacecraft observations and theoretical considerations (Krasnopolsky, 2005).

Satellite and ground-based observations indicate that the martian atmospheric CH₄ is not uniformly mixed, but concentrated in the equatorial region relative to the polar regions (Mumma *et al.*, 2004). Since the horizontal mixing time for the martian atmosphere is ~0.5 years (Krasnopolsky *et al.*, 2004b), this would imply that a CH₄ removal process more rapid than photochemical destruction must also exist. The sink could be some undefined surface oxidation phenomena or biological CH₄ oxidation equivalent to aerobic methanotrophy (CH₄ + 2O₂ → CO₂ + 2H₂O) in terrestrial microorganisms that rely on the trace O₂ in the martian atmosphere [~1,300 parts per million (ppmv) or ~7 × 10⁷ mol (Owen, 1992)]. Regardless of the mechanisms, the spatial heterogeneity in the CH₄ atmospheric abundance implies that the subsurface CH₄ flux could be much greater than the ~2 × 10⁵ cm⁻² s⁻¹ required by the photochemical loss rate. An estimated flux is given by the following:

$$F = \Delta C M_a A / (S_M \tau s_{yr})$$

where ΔC is the range in CH₄ concentration ~100 × 10⁻⁹, M_a is the martian atmosphere = 5.4 × 10¹⁷ mol, A is Avogadro's number = 6.02 × 10²³ atoms mol⁻¹, S_M is the surface area of Mars = 0.4 × 10¹⁸ cm², τ is the mixing time in the Martian atmosphere = 0.5 year, and s_{yr} = 3.2 × 10⁷ s year⁻¹. This expression yields an estimated CH₄ flux of 2 × 10⁹ cm⁻² s⁻¹. The H₂ required to produce the CH₄ could originate in the martian atmosphere by photochemical destruction of H₂O producing 15 ppmv of H₂, which in turn could diffuse into the regolith at a rate of 9 × 10⁹ cm⁻² s⁻¹ (Summers *et al.*, 2002). Given the 4:1 stoi-

chiometric ratio of H to C, a 2 × 10⁹ cm⁻² s⁻¹ CH₄ flux should significantly deplete the H₂ concentration of the martian atmosphere.

This article examines whether an alternative CH₄ source—abiogenic CH₄—and an alternative H₂ source—radiolytic H₂ produced in the martian crust—could sustain the recently reported subsurface CH₄ flux. This study first demonstrates the importance of both abiogenic CH₄ and radiolytic H₂ as the source of CH₄ flux in the South African Precambrian crust of the Witwatersrand Basin. This 2.9–2.5 × 10⁹ year old (Ga) basin has not experienced volcanism in 200 × 10⁶ years (Myr), and previous reports indicate that subsurface microbial communities are sustained by subsurface generation of H₂ through radiolysis of water (Lin *et al.*, 2005b; Sherwood Lollar *et al.*, 2005). A coupled reaction and diffusive transport model of this basin calibrated by He flux is used to model He, H₂, and CH₄ in the martian subsurface and determine whether their rates can explain the estimated martian subsurface CH₄ flux. Four different origins for martian CH₄ are discussed in the context of this model: (1) volcanogenic; (2) sublimation of hydrate-rich ice; (3) diffusive transport through hydrate-saturated cryosphere; and (4) microbial CH₄ generation above the cryosphere. This article concludes with a discussion as to how to distinguish between the different CH₄ sources and what is the most capable analytical technology for characterizing the martian CH₄ in future rover missions.

CH₄ IN PRECAMBRIAN SHIELDS

Isotopic composition of CH₄–C₄H₁₀ and abiogenic CH₄

To date, the characteristics of abiogenic hydrocarbons on Earth have not been well defined. The earliest reported abiogenic CH₄ occurrences were those identified by Welhan *et al.* (1979), which were discharging at the East Pacific Rise and very ¹³C-rich due to their mantle-derived carbon source. Mantle-derived carbon sources have also been invoked to explain the ¹³C-enriched CH₄ produced by serpentinization at the Zambales ophiolite sequence (Abrajano *et al.*, 1988, 1990) and the Lost City Hydrothermal Field (Kelley *et al.*, 2005) (Fig. 1).

Not all abiogenic CH₄ is mantle in origin. In continental crust, such as Precambrian Shield

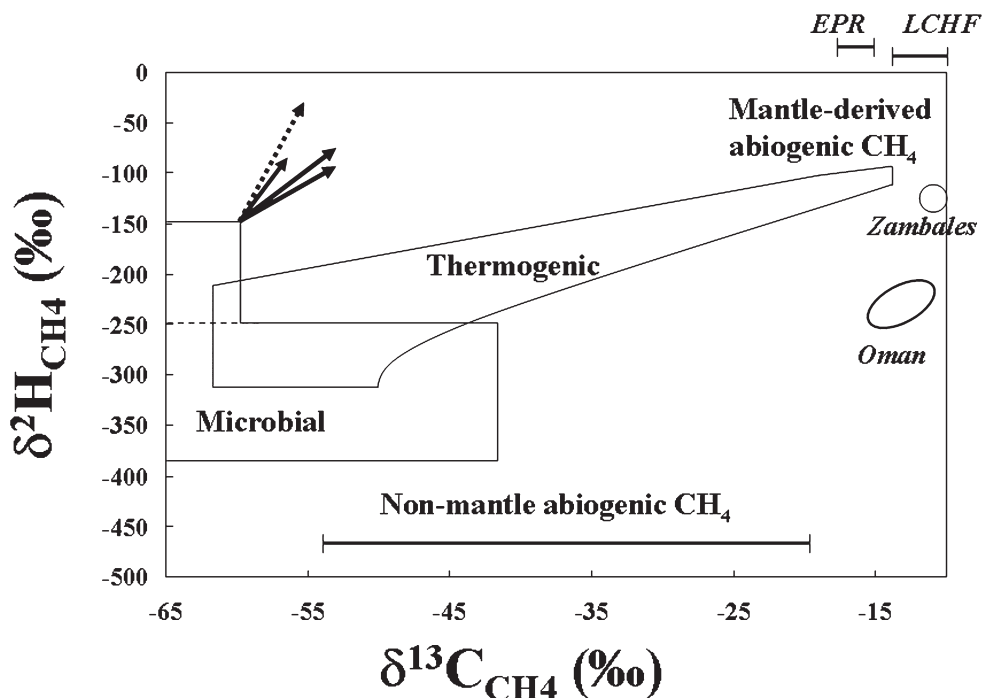


FIG. 1. C and H isotopic signatures for thermogenic, microbial, and abiogenic sources of CH₄ (adapted from Schoell, 1988). The range of $\delta^{13}\text{C}$ values for suggested abiogenic CH₄ varies significantly depending on local carbon source. Where mantle carbon sources are invoked, highly enriched $\delta^{13}\text{C}$ values have been reported, e.g., East Pacific Rise (EPR) (Welhan and Craig, 1979), serpentinization-related CH₄ from the Lost City Hydrothermal Field (LCHF) (Kelley *et al.*, 2005), Zambales (Abrajano *et al.*, 1988), and Oman ophiolite sequences (Fritz *et al.*, 1992). Abiogenic CH₄ produced by non-mantle carbon sources produces a wide range of $\delta^{13}\text{C}$ values as shown in experiments (Horita and Berndt, 1999) and Precambrian Shield field site studies (Sherwood Lollar *et al.*, 1993a, 2002, 2005). For some of these studies, only ^{13}C values are available so a range of ^{13}C values (horizontal lines) rather than plotted data are shown for comparison. The black arrows represent the stable isotope fractionation trend produced by aerobic methanotrophy (Coleman *et al.*, 1981; Reeburgh, 2003), the gray arrows represent anaerobic methanotrophy (Alperin *et al.*, 1988; Reeburgh, 2003), and the dashed arrow represents photochemical destruction of CH₄ (Nair *et al.*, 2005).

rocks, processes of gas–water–rock interaction, including serpentinization, Fischer-Tropsch synthesis ($3\text{H}_2 + \text{CO} = \text{CH}_4 + \text{H}_2\text{O}$), and the metamorphism of carbonate–graphite-bearing rocks ($2\text{H}_2\text{O} + 2\text{C} = \text{CH}_4 + \text{CO}_2$) produce abiogenic hydrocarbons. This abiogenic CH₄ possesses ^{12}C -rich signatures isotopically lighter than that of mantle-derived CH₄ and reflects local crustal carbon sources (Sherwood Lollar *et al.*, 1993a, 2005). Similarly, hydrothermal laboratory experiments have yielded CH₄ depleted in ^{13}C with a $\delta^{13}\text{C}$ -67% Vienna Pee Dee Formation Belemnite standard (VPDB) relative to the source CO₂ (Horita and Berndt, 1999) (Fig. 1).

A more rigorous test for distinguishing microbial from abiogenic hydrocarbons moves beyond comparing absolute $\delta^{13}\text{C}$ values of the CH₄ to examining the pattern of stable isotope variation among CH₄, C₂H₆, C₃H₈, and C₄H₁₀, as was done for the Murchison meteorite (Yuen *et al.*, 1984)

and abiogenic hydrocarbons produced in spark discharge experiments (Des Marais *et al.*, 1981). Substantial volumes of CH₄ gas are discharged from fractures and boreholes throughout the Precambrian Shield rocks of Canada, Fennoscandia, and South Africa (Ward *et al.*, 2004; Sherwood Lollar *et al.*, 1993a, 2002, 2005). Based on measurements of the ^{13}C and ^2H isotope variations in CH₄ and higher hydrocarbons in Precambrian Shield rock gases, Sherwood Lollar *et al.* (2002, 2005) proposed that an isotopic pattern of C isotope depletion in ^{13}C and H isotope enrichment in ^2H from CH₄ to C₄H₁₀ was characteristic of abiogenically produced gases. This is based on the hypothesis that during polymerization of CH₄ to produce higher hydrocarbons there will be a preferential rate of reaction for the light isotopes, which results in the preferential incorporation of ^{12}C into the products of the reaction concomitant with a preferential loss of ^1H (Fig. 2).

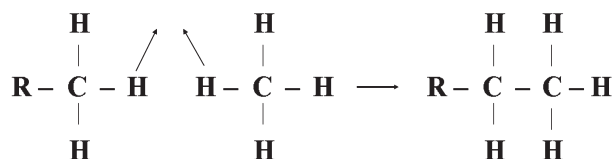


FIG. 2. The proposed carbon and hydrogen isotope fractionation process during abiogenic polymerization of C_2H_6 from CH_4 . With C addition, a preferential rate of reaction for ^{12}C leads to ^{13}C -depleted ethane [carbon isotope hypothesis from Des Marais *et al.* (1981)]. With H elimination, a preferential rate of reaction for ^1H leads to ^2H -enriched ethane [hydrogen isotope hypothesis from Sherwood Lollar *et al.* (2002)].

In the case of the 2.9-Ga Witwatersrand Basin of South Africa, the deep Au mines provide a unique opportunity to examine the regional distribution (350×150 km) and vertical distribution

(up to 3.3 km depth) of CH_4 sources and sinks. The data have provided the first picture of the CH_4 cycle for stable, Precambrian continental crust that has not experienced recent volcanic activity.

The isotopic composition and concentration of H_2 , He, and CH_4 to C_4H_{10} hydrocarbons and the sequences of the 16S rDNA were determined for fracture water samples collected at depths ranging from 0.2 to 3.3 km from the Witwatersrand Basin, South Africa (Lippmann *et al.*, 2003; Ward *et al.*, 2004; Onstott *et al.*, 2005). Samples were collected from the southernmost Welkom (shaded squares in Figs. 3–5), easternmost Evander (shaded diamonds in Figs. 3–5), and northernmost Carletonville (shaded triangles in Figs. 3–5) mining regions and from the overlying 2.45-Ga Transvaal

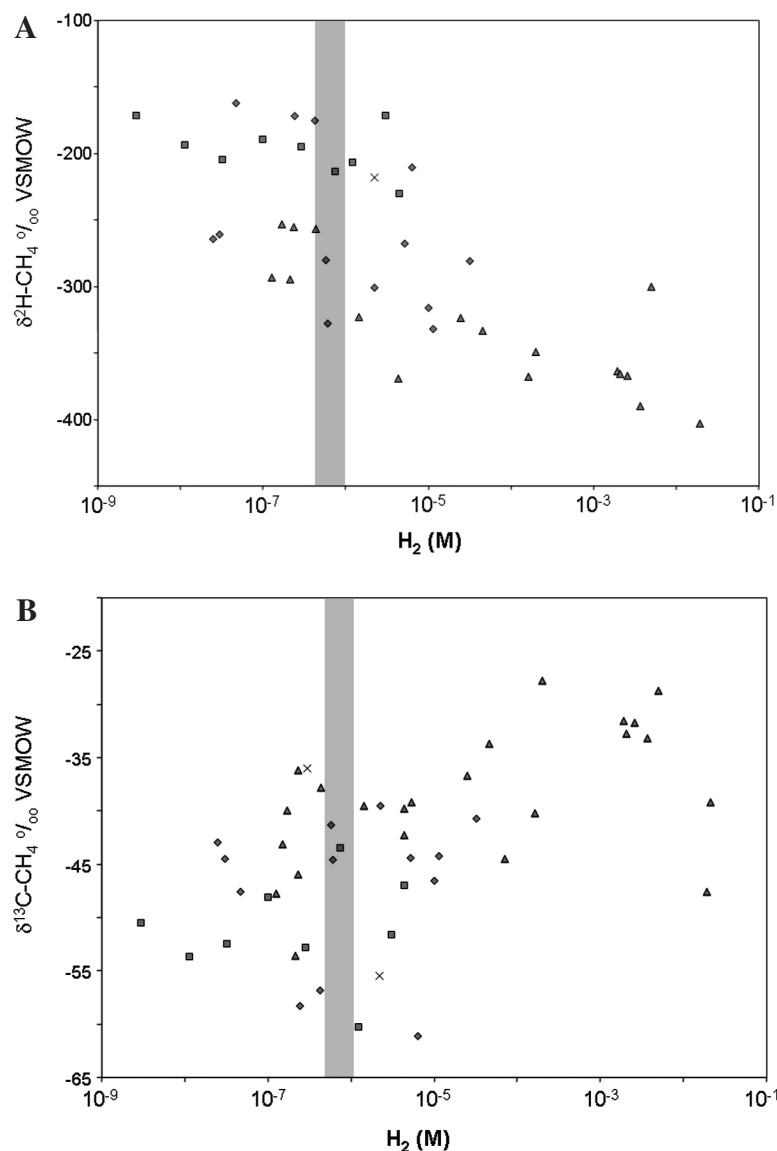
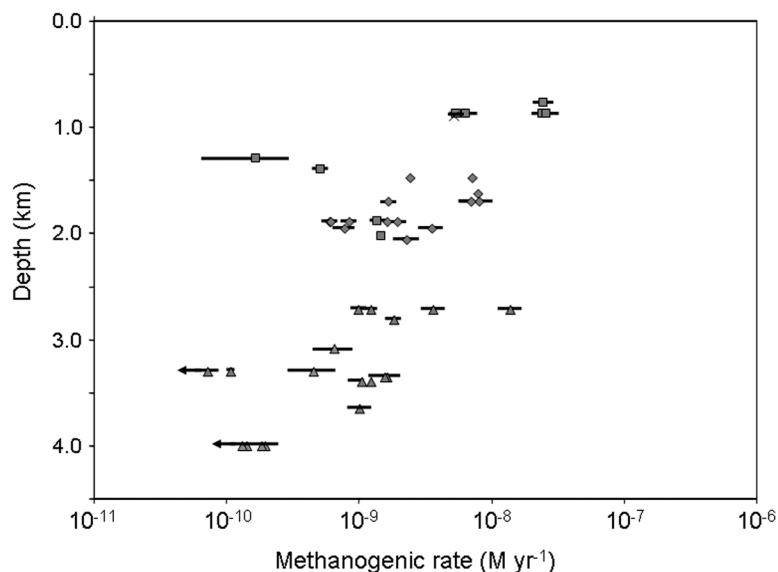


FIG. 3. A: $\delta^2\text{H}$ of CH_4 versus H_2 concentration for fracture water samples from the Witwatersrand Basin, South Africa. Samples were collected from the Welkom (shaded squares), Evander (shaded diamonds), and Carletonville (shaded diamonds) mining regions and from the overlying 2.45-Ga Transvaal dolomitic aquifer (\times). Correlation coefficient is 0.58. B: $\delta^{13}\text{C}$ of CH_4 versus H_2 concentration for fracture water samples from the Witwatersrand Basin, South Africa. Correlation coefficient is 0.32. Gray rectangle delineates the H_2 concentration range for which the ΔG of the reaction $4\text{H}_2 + \text{H}^+ + \text{HCO}_3^- \rightarrow \text{CH}_4 + 3\text{H}_2\text{O}$ equals -20 kJ mol^{-1} . The ΔG is more negative to the right of the gray rectangle and less negative to the left of the gray rectangle.

FIG. 4. Methanogenic rate calculated from isotope model (see text for details) versus depth. Samples were collected from the Welkom (shaded squares), Evander (shaded diamonds), and Carletonville (shaded diamonds) mining regions and from the overlying 2.45-Ga Transvaal dolomitic aquifer (×). Error bars represent 1 standard deviation from the average of three different estimates for the methanogenic rate from Eqs. 1, 3 and 4 in the text. Arrows indicates maximum estimate of methanogenic rate tolerated by the isotopic data.



dolomitic aquifer (crosses in Figs. 3–5) and the 250-Ma Karoo coal seams (asterisk in Fig. 4).

As reported by Ward *et al.* (2004) and Sherwood Lollar *et al.* (2005), the CH₄ of the Witwatersrand Basin represents a mixture of methanogenic CH₄ and abiogenic CH₄. Microbially produced CH₄ was characterized by relatively depleted $\delta^{13}\text{C}$ values, enriched $\delta^2\text{H}$ values, and CH₄/C₂+ (C₂+ = ethane + propane + butane) values on the order of 10³–10⁵ (Schoell, 1988; Hunt, 1996). In contrast, the abiogenic component had substantially more C₂+ relative to CH₄, with CH₄/C₂+ ratios typically <100, and relatively enriched $\delta^{13}\text{C}$ values and depleted $\delta^2\text{H}$ values. Where microbial CH₄ was prevalent, 16S rDNA analyses generally confirmed the presence of methanogenic, sometimes autotrophic, microorganisms (Ward *et al.*, 2004).

Many of the Precambrian Shield sites contain substantial concentrations of H₂ (up to 5 mM) and He in addition to hydrocarbon gases (Sherwood Lollar *et al.*, 1993a, 2005). Sampling of the same boreholes over several years has shown that the high H₂ levels are not an artifact of drilling but a persistent natural phenomenon in this environment (Sherwood Lollar *et al.*, 1993b, 2002). The high He concentrations are caused by the radioactive decay of U and Th (Lippmann *et al.*, 2003). Like the hydrocarbon gases, the high quantities of H₂ are likely the product of abiogenic water–rock interactions in these highly impermeable, high rock-to-water ratio environments. Specific H₂-generating reactions may vary from

one geological environment to another, ranging from serpentinization reactions in ultramafic rock (Abrajano *et al.*, 1990) to radiolytic decomposition of water in the U-rich continental crust (Lin *et al.*, 2005a,b). The association of high H₂ concentrations with a ¹³C-enriched CH₄ component and low H₂ concentrations with the ¹³C-depleted methanogenic component in South Africa suggests that H₂-driven autotrophy supports methanogenesis in the deep subsurface (Sherwood Lollar *et al.*, 2005).

For Witwatersrand Basin fluids, the relationship between H₂ concentration and the $\delta^2\text{H}$ and $\delta^{13}\text{C}$ values for CH₄ is particularly pronounced (Fig. 3). The fracture water with dominantly abiogenic CH₄ contained millimolar H₂ concentrations, whereas fracture water with dominantly methanogenic CH₄ yielded micromolar H₂ concentrations. The presence of methanogenic CH₄ with H₂ concentrations greater than 10 nM is still consistent with autotrophic methanogenesis. Though CO₂—the dominant electron acceptor—is limited, the environment is not H₂ limited (Onstott *et al.*, 2005). The minimal energy yield necessary for ATP synthesis (–20 kJ mol⁻¹) (Shink, 1997) requires H₂ concentrations of at least 500–1,000 nM. This is not the case in marine sediments (Hoehler *et al.*, 1998).

In situ rates of microbial CH₄ production and the abiogenic CH₄ flux

The CH₄ concentration, isotopic composition, and surface flux for the South African crust were

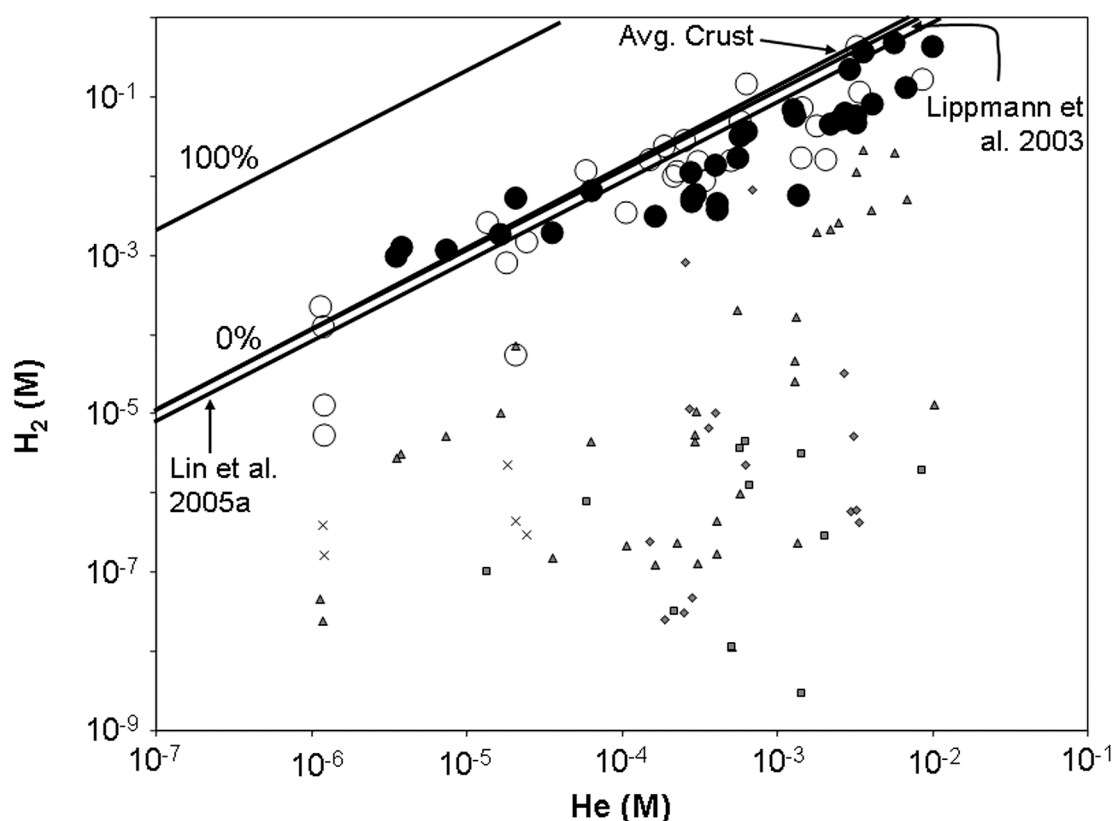


FIG. 5. H_2 versus He concentration for fracture water samples from the Witwatersrand Basin, South Africa. Samples were collected from the Welkom (shaded squares), Evander (shaded diamonds), and Carletonville (shaded diamonds) mining regions and from the overlying 2.45-Ga Transvaal dolomitic aquifer (\times). H_2 concentrations that have been corrected for loss to CH_4 by methanogenesis (open circles) and for loss to C_1 – C_4 hydrocarbons by abiotic processes (solid circles) are also plotted for comparison (see text for details). The trend marked Avg. Crust represents the predicted H_2 concentration from radiolysis of pore water (Spinks and Woods, 1990) and the He concentration in the pore water assuming that 0% of the α particles from U and Th decay are retained by the mineral phases and that all of them diffuse into the pore water from the continental crust with 1% porosity and K, U, and Th concentrations of 3.4%, 2.8 ppm, and 10.8 ppm, respectively. The trend marked Lippmann et al. 2003 represents the predicted H_2 yield from radiolysis of pore water for continental crust with 1% porosity and K, U, and Th concentrations of 3.4%, 520 ppm, and 10.8 ppm, respectively. The trend marked Lin et al. 2005a represents the predicted H_2 concentration from radiolysis of pore water using the same crustal composition as Lippmann et al. (2003) but with the experimentally determined H_2 yield of Lin et al. (2005a). The trend marked 100% is the same as the Average Crust trend, but assumes that 100% of the α particles released within the mineral phases are retained and not lost by diffusion to the pore water.

modeled using an approach similar to that employed by Lippmann et al. (2003) to determine the He age of fracture water and interpret the H_2 and CH_4 data. The modeled CH_4 concentration, tCH_4 , assumed to represent the sum of abiogenic CH_4 flux and microbial CH_4 generated *in situ*, is given by:

$${}^tCH_4 = {}^{He}t\{[J_{CH_4}/(\theta\rho_w z)] + [P_{CH_4}]\} \quad (1)$$

where J_{CH_4} is the abiogenic CH_4 flux ($\text{mol dm}^{-2} \text{ year}^{-1}$), θ is the porosity (0.5–2%), z is depth (dm), P_{CH_4} is the rate of methanogenesis ($M \text{ year}^{-1}$), and

${}^{He}t$ is the He age of the fracture water and is given by the equation from Lippmann et al. (2003):

$${}^{He}t = [He]/\{[J_{He}/(\theta\rho_w z)] + [\gamma He(1 - \theta\rho_r/\theta\rho_w)P_{He}]\} \quad (2)$$

where $[He]$ is the measured He concentration in the fracture water, J_{He} is the He flux, ρ_w is the fracture water density, ρ_r is the rock matrix density, γHe is the fraction of He produced in the minerals that is released into the pore water, and P_{He} is the *in situ* production rate of He. For the Witwatersrand Basin, Lippmann et al. (2003) used

$J_{\text{He}} = 1.6 \times 10^{-8} \text{ mol dm}^{-2} \text{ year}^{-1}$ ($3.1 \times 10^6 \text{ cm}^{-2} \text{ s}^{-1}$), $\rho_w = 0.98\text{--}1.03 \text{ kg dm}^{-3}$, $\rho_r = 2.65\text{--}2.70 \text{ kg dm}^{-3}$, and $P_{\text{He}} = 7.6 \times 10^{-12}\text{--}7.4 \times 10^{-10} \text{ mol dm}^{-3} \text{ year}^{-1}$ ($1.5 \times 10^2\text{--}1.4 \times 10^4 \text{ cm}^{-3} \text{ s}^{-1}$). The range in P_{He} reflects the range in U concentrations in the rock strata. We calculated that the γ_{He} is $\sim 0.6\%$, given the 1% porosity (*i.e.*, the mean free path of the α particle, 10–50 μm , greatly exceeds that of the rock pore size, $<0.15 \mu\text{m}$ based upon Hg porosimetry data) and the relatively lower stopping power of water compared with that of silicates. Lippmann *et al.* (2003) argued that γ_{He} is $\sim 100\%$, because the ambient temperature of the rock strata bounding the fractures ranged from 40°C to 60°C, a temperature range that falls within the closure temperature range of the U-bearing minerals (Shuster *et al.*, 2004). Lippmann *et al.* (2003) assumed that since the rock strata have been at this temperature range for $\sim 35 \text{ Myr}$ (Omar *et al.*, 2003), almost all of the He would have diffused out of the U-bearing mineral and into the pore water, making γ_{He} effectively $\sim 100\%$.

The microbial CH₄ production rate was also constrained by the isotopic composition of the CH₄, which is given by the following expressions:

$$\delta^2\text{H} - \text{CH}_4 = {}^{\text{He}t} \times \{ [J_{\text{CH}_4} / (\theta \rho_w z) \times \delta^2\text{H}_{\text{CH}_4\text{A}}] + [P_{\text{CH}_4} \times \delta^2\text{H}_{\text{CH}_4\text{B}}] \} / T_{\text{CH}_4} \quad (3)$$

$$\delta^{13}\text{C} - \text{CH}_4 = {}^{\text{He}t} \times \{ [J_{\text{CH}_4} / (\theta \rho_w z) \times \delta^{13}\text{C}_{\text{CH}_4\text{A}}] + [P_{\text{CH}_4} \times \delta^{13}\text{C}_{\text{CH}_4\text{B}}] \} / T_{\text{CH}_4} \quad (4)$$

where $\delta^2\text{H}_{\text{CH}_4\text{A}}$ and $\delta^{13}\text{C}_{\text{CH}_4\text{A}}$ are the isotopic compositions of the abiogenic CH₄ component (Fig. 3) and $\delta^2\text{H}_{\text{CH}_4\text{B}}$ and $\delta^{13}\text{C}_{\text{CH}_4\text{B}}$ are the isotopic compositions of the microbial CH₄ (Fig. 3). Equations 1, 3, and 4 were solved simultaneously for the P_{CH_4} for each sample, the abiogenic CH₄ flux J_{CH_4} , and the isotopic composition of the microbial and abiogenic CH₄. The data were best fit ($\chi^2 = 0.2$) by an abiogenic CH₄ isotopic composition of $\delta^2\text{H}_{\text{CH}_4\text{A}} = -360\text{‰}$ and $\delta^{13}\text{C}_{\text{CH}_4\text{A}} = -30\text{‰}$; a microbial CH₄ isotopic composition of $\delta^2\text{H}_{\text{CH}_4\text{B}} = -220\text{‰}$ and $\delta^{13}\text{C}_{\text{CH}_4\text{B}} = -65\text{‰}$; and an abiogenic CH₄ flux of $8.9 \times 10^{-8} \text{ mol dm}^{-2} \text{ year}^{-1}$ ($1.8 \times 10^7 \text{ cm}^{-2} \text{ s}^{-1}$). For these model parameters the *in situ* microbial CH₄ production rates ranged from $<10^{-10}$ to $10^{-7} \text{ mol dm}^{-3} \text{ year}^{-1}$ ($<2 \times 10^3$ to $2 \times 10^6 \text{ cm}^{-3} \text{ s}^{-1}$). The lowest rates represent maximum estimates for the deepest CH₄ gas samples, which were isotopi-

cally indistinguishable from abiogenic CH₄. Despite the fact that the fracture water samples come from three different mining regions that are separated by a distance of hundreds of kilometers and encompass a wide range of aqueous geochemical compositions, the methanogenic rates from different regions overlapped when plotted versus depth and displayed an exponential decline with depth (Fig. 4).

The slow rates of methanogenesis from CO₂ reduction and H₂ consumption imply a long-term H₂ source. When H₂ concentrations were compared with that of He for fracture water samples from the Witwatersrand Basin (Fig. 5), the H₂ concentration exhibited no obvious correlation with the fracture water age. When H₂ concentrations were corrected, however, for the loss to CH₄ by methanogenesis (open circles in Fig. 5) and for loss to C₁–C₄ hydrocarbons by abiogenic processes (solid circles in Fig. 5), they exhibited a distinct positive correlation with He concentrations, *i.e.*, the H₂ concentrations increased as the fracture water age increased. Lin *et al.* (2005b) have shown that these corrected H₂ concentrations are consistent with a radiolytic source mechanism for the H₂. The He effectively acts as a dosimeter for the α dose if one assumes that 0% of the He generated by the decay of U- and Th-bearing minerals remains in the minerals ($\gamma_{\text{He}} = 1$). The predicted trend is not significantly altered whether one uses the radiolytic yield for pure oxygenated water (Spinks and Woods, 1990) or that of saline anaerobic water (marked as Lin *et al.*, 2005a in Fig. 5). Nor do drastic variations in the (U + Th)/K ratio of the rock from 7×10^{-9} to 3×10^{-7} (Lippmann *et al.*, 2003) significantly affect the predicted H₂ versus He trend even though they do affect the production rates. Variations in the porosity between 0.01% and 5% change the relative production rates of H₂ and He by less than 10%. The relationship between H₂ and He is affected, however, by how much He is retained by the U-bearing minerals. If 100% of the α particles released within the mineral phases are retained and not lost by diffusion to the pore water then the H₂/He ratio increases by ~ 100 (100% in Fig. 5).

He-, H₂-, and CH₄-coupled flux model for South Africa

To determine whether the radiolytic production of H₂ was sufficient to support the observed

in situ microbial CH₄ production rates, the subsurface fluxes of He, H₂, and CH₄ were modeled for a 5-km-thick crust with diffusive flux coupled to *in situ* generation and consumption (MatLab version 7.1, The MathWorks, Inc., Natick, MA). The diffusion parameter for He in water was derived from Lippmann *et al.* (2003), and the diffusion parameters for H₂ and CH₄ in water were obtained from Cussler (1985) (Table 1). The matrix diffusivities were corrected for a porosity that varied with depth exponentially from a maximum of 2% and an e^{-1} decay parameter of 1.5 km. The diffusivities in water were also corrected for temperature and water viscosity using the geothermal gradient of 10°C km⁻¹ (Omar *et al.*, 2003). The kilometer scale diffusivity was treated as a 50:50 mixture of diffusion through water and matrix diffusion by the following approximation:

$$D_{\text{bulk}} = 0.5 \theta D_w + 0.5 D_w$$

This expression emulates fast diffusion through interconnected fracture networks with a fracture spacing of ~100 m and follows the He gas transport models of the Stripa granite (Andrews *et al.*, 1989). The surface concentrations of He, H₂, and CH₄ were assumed to be zero.

Three models for He *in situ* generation and basal flux were tested. The first model is from Lippmann *et al.* (2003), has no basal flux of He, and relies strictly upon an He *in situ* generation rate of 3.2×10^{-13} mol dm⁻³ year⁻¹ (Table 1), which corresponds to an average U concentration of 20 ppm and yields fracture water ages of tens to hundreds of millions of years. The second model is also from Lippmann *et al.* (2003) and uses a basal He flux of 1.6×10^{-8} mol dm⁻² year⁻¹ (3.1×10^6 cm⁻² s⁻¹) and an He *in situ* generation rate of 4.2×10^{-12} mol dm⁻³ year⁻¹ (Table 1), which corresponds to an average U concentration of 300 ppm and yields fracture water

ages of 1 to tens of millions of years (marked as Lippmann *et al.*, 2003 in Fig. 5). The third model utilizes an He *in situ* generation rate of 7.6×10^{-14} mol dm⁻³ year⁻¹ (Table 1), which corresponds to an average continental crust U concentration of 3 ppm and a basal He flux of 8.9×10^{-8} mol dm⁻² year⁻¹ (1.5×10^5 cm⁻² s⁻¹), and yields fracture water ages very similar to the second model (marked as Avg. Crust in Fig. 5). A Th concentration of the average continental crust (10.4 ppm) was used for all three models. In all three models the release of He from the mineral matrix was increased from 0.6% to 100% to simulate diffusive loss from the minerals to the pore water as the temperature increased with depth from 20°C to 70°C.

The CH₄ mixing model was evaluated for all three models. Because the second and third model yielded similar ^{He}*t*, their basal CH₄ flux was set equal to the 8.9×10^{-8} mol dm⁻² year⁻¹ abiogenic CH₄ flux derived in the calculations above, which were based upon the He parameters of the second model (Table 1). The first model, which possessed much greater ^{He}*t* values, yielded a lower abiogenic flux of 2.2×10^{-9} mol dm⁻² year⁻¹ (4.4×10^3 cm⁻² s⁻¹).

A least squares fit of the data in Fig. 4 yielded the following expression for the *in situ* microbial CH₄ generation rate:

$$P_{\text{CH}_4} \text{ (mol dm}^{-3} \text{ year}^{-1}\text{)} = 1.2 \times 10^{-10} e^{(-0.0005z)} \quad (5)$$

For the third model the expression was $3.0 \times 10^{-10} e^{(-0.0010z)}$. For the first model with the much greater ^{He}*t* values, the *in situ* microbial CH₄ generation rate was much less, $5.4 \times 10^{-12} e^{(-0.0004z)}$ (Table 1).

The basal H₂ flux was assumed to be zero. The *in situ* radiolytic H₂ generation rate was based on the model of Lin *et al.* (2005a), the radiolytic H₂

TABLE 1. MODEL PARAMETERS FOR THE SOUTH AFRICAN CRUST

Species	D_w m ² year ⁻¹	Model	In situ production rate (mol dm ⁻³ year ⁻¹)	Basal flux (mol dm ⁻² year ⁻¹)
He	$25.8 e^{[-11,700/(7.948 \times T)]}$	1	3.2×10^{-13}	0
		2	4.2×10^{-12}	1.6×10^{-8}
		3	7.6×10^{-14}	8.9×10^{-8}
H ₂	$4.35 \times 10^{-13} T / (6\pi\mu 5.45 \times 10^{-9})^a$	1	3.2×10^{-11}	0
		2	4.2×10^{-10}	0
		3	8.6×10^{-12}	0
CH ₄	$4.35 \times 10^{-13} T / (6\pi\mu 1.65 \times 10^{-8})$	1	$5.4 \times 10^{-12} e^{(-0.0004z)}$	2.2×10^{-9}
		2	$1.2 \times 10^{-10} e^{(-0.0005z)}$	8.9×10^{-8}
		3	$3.0 \times 10^{-10} e^{(-0.0010z)}$	8.9×10^{-8}

^a μ = viscosity of water at temperature *T*.

yield of Lin *et al.* (2005a), the U and Th concentrations for the three models stated above, the K concentration for the average continental crust of 3.4%, and the porosity stated above. The *in situ* radiolytic H₂ generation rates ranged from 8.6×10^{-12} mol dm⁻³ year⁻¹ for the first model (lowest U content) to 4.2×10^{-10} mol dm⁻³ year⁻¹ for the second model (highest U content) (Table 1). The model also assumed that the *in situ* H₂ consumption rate was four times that of the *in situ* microbial CH₄ production rate given the reaction stoichiometry.

The second and third models yielded a (H₂ + CH₄)/He concentration ratio of ~50, whereas the first model yielded a (H₂ + CH₄)/He concentration ratio of ~75. Both values are consistent with the observed trend in (H₂ + CH₄)/He (Fig. 5). Not surprisingly, the model results indicated that the *in situ* He generation rate in the top 5 km accounted for 99% of the surface flux of He, which varied from 1×10^{-8} to 5×10^{-7} mol dm⁻² year⁻¹ (2×10^6 – 1×10^8 cm⁻² s⁻¹) for models 3 and 2, respectively. The *in situ* microbial CH₄ production rates increased the surface CH₄ flux to $\sim 10^{-7}$ to 10^{-5} mol dm⁻² year⁻¹ (2×10^7 – 2×10^9 cm⁻² s⁻¹) for models 1 and 3, respectively. The model also demonstrated that the *in situ* H₂ generation rate more than sufficed to support the estimated microbial CH₄ production rates and still yielded a surface flux of $\sim 10^{-6}$ – 5×10^{-5} mol dm⁻² year⁻¹ (2×10^8 – 1×10^{10} cm⁻² s⁻¹) for models 3 and 2, respectively. Obviously such a surface flux is not observed as other electron-accepting microbial reactions quickly consume the H₂. It is also possible that the abiogenic CH₄ is not rising from a deeper, hotter source as assumed in our model, but is forming within the upper 5 km of South African crust. Finally, the modeled CH₄ surface flux has to be considered a minimum estimate because our original model did not attempt to quantify any CH₄ oxidation rates even though the 16S rDNA sequences for both aerobic and anaerobic methane oxidizers have been detected in the shallowest groundwater boreholes.

RELEVANCE TO THE ORIGIN OF MARTIAN CH₄

As a conservative tracer, He provides a means of relating our South African crustal model to the conditions on Mars. The He abundance in the lower martian atmosphere was originally estimated to be ~1 ppm with an average lifetime of 5×10^4 years due to loss to space at a rate of 1.8×10^5 cm⁻² s⁻¹ (1.4×10^7 mol year⁻¹) (Krasnopolsky *et al.*, 1994). This loss rate was presumed to be balanced by a subsurface flux of comparable value. Krasnopolsky and Gladstone (1996) revised the He abundance upward to $\sim 4 \pm 2$ ppm, but kept the same subsurface flux and calculated an average lifetime of 13×10^4 years (Krasnopolsky and Gladstone, 2005) while invoking an additional solar α flux to explain the greater He abundance in the martian atmosphere. Recent papers that seek to constrain the origin of the martian CH₄ have ignored He subsurface flux from the martian crust (Krasnopolsky, 2005; Krasnopolsky and Gladstone, 2005), citing the lack of recent volcanism as justification for this assumption. Significant crustal He flux in the absence of volcanism has been documented for many places on Earth, including the South African Precambrian shield (Lippmann *et al.*, 2003). For the remainder of this paper we will assume that the modeled martian He subsurface flux of 1 – 3×10^5 cm⁻² s⁻¹ (1 – 3×10^7 mol year⁻¹) (Krasnopolsky and Gladstone, 1996) is still applicable.

In the Witwatersrand Basin, the ratio of the surface abiogenic CH₄ flux to He surface flux varied from ~10 to 1 in the three models. If we apply the same ratios to the martian subsurface He flux, the corresponding martian subsurface abiogenic CH₄ flux would be $\sim 2 \times 10^5$ – 2×10^6 cm⁻² s⁻¹ (0.2 – 1.5×10^8 mol year⁻¹). Although this flux can sustain the photochemical loss rate of CH₄ from the martian atmosphere, it is less than the $\sim 2 \times 10^9$ cm⁻² s⁻¹ of subsurface CH₄ flux required by the nonuniform CH₄ concentrations. If one considers the combined abiogenic and microbial South African CH₄ flux, the CH₄/He flux ratio is 10–20, and the corresponding martian CH₄ flux would be 2 – 4×10^6 cm⁻² s⁻¹ (1.5 – 3.0×10^8 mol year⁻¹).

For abiogenic CH₄ generated by serpentinization of modern or ancient ocean crust, the ratio of CH₄ and H₂ to He ranges from ~200 to 200,000 (Fig. 6) (Abrajano *et al.*, 1988; Seyfried and Mottl, 1995). By applying this ratio to the martian subsurface He flux, the corresponding martian subsurface abiogenic CH₄ flux would be $\sim 2.5 \times 10^7$ – 5.0×10^{10} cm⁻² s⁻¹ (1.9×10^9 – 3.8×10^{12} mol year⁻¹). Oxidation of Fe-bearing olivine or pyroxene in basalt by water can potentially generate significant H₂ that could sustain abiogenic and microbial CH₄ production (Stevens and McKinley, 1995; Wallendahl and Treiman, 1999). The rates for these reactions increase with temperature in the presence of liquid H₂O (Oze and

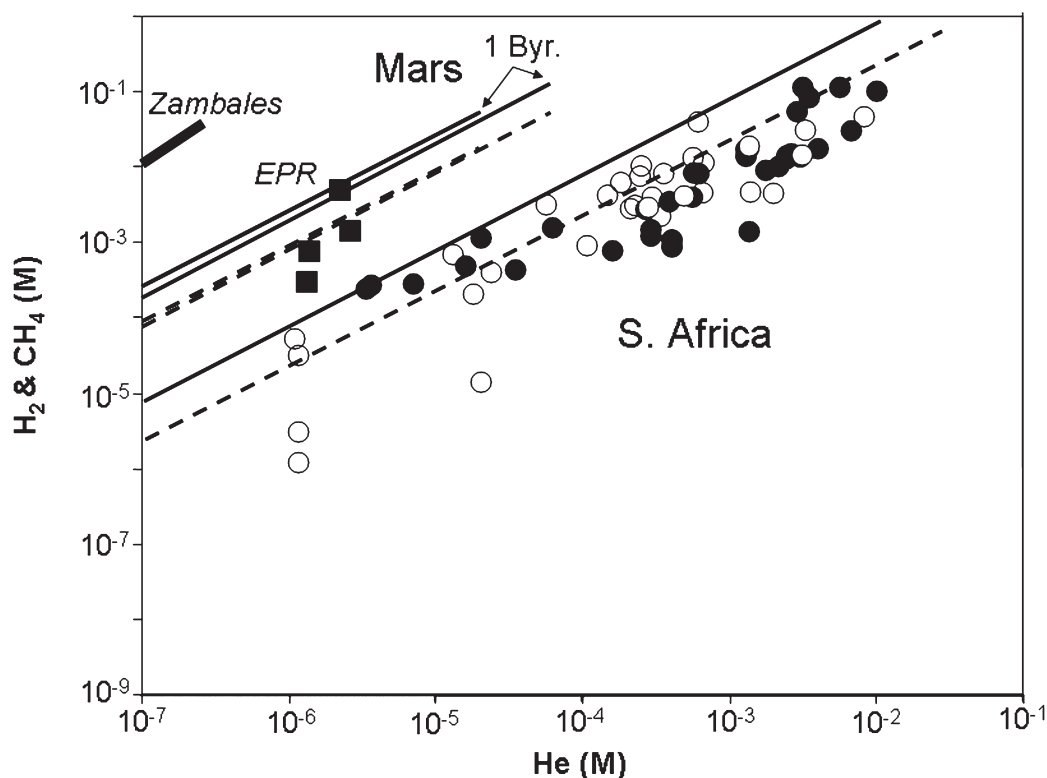


FIG. 6. H_2 and CH_4 versus He for fracture water samples from the Witwatersrand Basin, South Africa. H_2 concentrations that have been corrected for loss to CH_4 by methanogenesis (open circles) and for loss to $\text{C}_1\text{--C}_4$ hydrocarbons by abiotic processes (solid circles) are also plotted for comparison (see text for details). Solid squares represent the $\text{H}_2 + 2\text{xCH}_4$ versus He concentrations of deep sea vent samples from the East Pacific Rise (EPR) and Endeavor (Seyfried and Mottl, 1995). Thick solid line labeled Zambales represents the $\text{H}_2 + 2\text{xCH}_4$ versus He ratio for the Zambales ophiolite (Abrajano *et al.*, 1988). Solid lines represent the H_2 versus He trends predicted by the radiolytic model. The dashed lines represent the $\text{H}_2/4 = \text{CH}_4$ concentrations. Byr, billion years.

Sharma, 2005) deeper in the martian crust. With increasing depth, however, H_2O becomes less abundant because of diminishing porosity, and as found to be the case in South Africa, CO_2 is stripped from solution as calcite because of increasing pH and Ca^{2+} with depth (Onstott *et al.*, 2005). If the rates implied above were extrapolated over 4.5×10^9 years, the amount of H_2 required would correspond to the serpentinization of a 50-m–113-km-thick global basalt layer composed of 10% FeO and producing magnetite.

In situ rates of He, H_2 , and microbial CH_4 production

A direct extrapolation of rates may not be appropriate given the uncertainties in the origin of He in the martian atmosphere and given that our hypothesized source of H_2 is radiolysis of H_2O and the martian crust is much more mafic than that of southern Africa. Production of H_2 by ra-

diolysis, however, can occur within the cryosphere where H_2O ice and CO_2 are more abundant. To determine whether a radiolytic mechanism could generate sufficient H_2 to produce the CH_4 detected in the martian atmosphere, we applied the same numerical scheme for the He, H_2 , and CH_4 generation and diffusive transport to a 6.6-km-thick, martian crustal profile utilizing the model of Clifford (1993) and Clifford and Parker (2001). This model assumes that porosity varies as a function of depth according to the following expression:

$$\Phi(z) = \Phi(0) \exp(-z/2.82) \quad (6)$$

where the depth z is in km and $\Phi(0) = 0.35$ (Clifford and Parker, 2001). Since the martian CH_4 concentration is greatest in the equatorial regions of Mars (Mumma *et al.*, 2004), the thermal model of Clifford and Parker (2001) for the equator was used. For this model the porosity is filled with ice

from 0 to 2 km deep and with NaCl brine for the remaining 4.6 km (Clifford and Parker, 2001).

The U, Th, and K concentrations of the martian crust were assumed to be 0.1 ppm, 0.4 ppm, and 0.25 wt%, respectively based upon the compositions of SNC meteorites (Chen and Wasserburg, 1985) and Alpha Particle X-ray Spectrometer analyses of rock units exposed on Meridiani Planum (Rieder *et al.*, 2004). Based on these parameters, assuming an H₂O-saturated porosity and the Lin *et al.* (2005a) model, the *in situ* H₂ generation rate increased with depth from 5.6×10^{-12} to 2.8×10^{-11} mol dm⁻³ year⁻¹. The *in situ* He generation rate increased with depth from 1.5 to 4×10^{-15} mol m⁻³ year⁻¹ as porosity diminished and temperature increased. With a mean annual surface temperature of 218K and a 17K km⁻¹ thermal gradient, no significant He loss from minerals occurred until ~4.5 km. Thus the *in situ* He generation rate within the upper 6.6 km of martian crust is much less than that of the South African crust (Table 2), whereas the *in situ* H₂ generation rate is comparable to the South African crust despite the lower U and Th content because of the higher porosity of the martian crust. The H₂/He production ratios for the martian radiolytic model vary from 19,000 to 1,400 with increasing depth compared with ~100 for the Witwatersrand Basin (Tables 1 and 2 and Fig. 6).

For the *in situ* microbial CH₄ production rate, the same exponential decline with depth was used, but the pre-exponential term was initially assumed to be 10⁵ times less than that for South Africa based upon the correlation between metabolic rate and temperature reported by Price and Sowers (2004). This assumes that the methanogenic biodensity is the same for the subsurface of South Africa and Mars despite the differences in porosity and the presence of ice. The *in situ* microbial CH₄ rate was then arbitrarily in-

creased until the H₂ flux resulting from *in situ* radiolytic production could just sustain it at steady state.

Surface flux for He, H₂, and microbial CH₄

The He and H₂ molecular diffusivities through the upper 2 km of ice were derived from Ikeda-Fukazawa *et al.* (2002) and Strauss *et al.* (1994), respectively (Table 2). The molecular diffusivity of CH₄ in ice is not well established but considered comparable to that of He (Ikeda-Fukazawa *et al.*, 2002), so a value four times less than that of He was adopted given the larger molecular size (Table 2). The formulas used to calculate the molecular diffusivities of He, H₂, and CH₄ through the lower 4.6 km of pore water were the same as those used in the South African model (Table 1). As in the South African case, the crustal-scale diffusivity was considered a 50:50 mixture of fracture and matrix diffusion pathways.

The basal flux of He at 6.6 km was adjusted until the surface flux matched the modeled values of $\sim 10^5$ cm⁻² s⁻¹ (Krasnopolsky *et al.*, 1994) at steady state. The corresponding basal abiogenic CH₄ flux was set to 10 times more than the basal He flux based upon the South African gas compositions. The basal H₂ flux was assumed to be zero.

Surface concentrations for He, H₂, and CH₄ were approximated from the reported concentrations in the martian atmosphere and Henry's law coefficients for He, H₂, and CH₄ derived from Smith and Kennedy (1983), Gordon *et al.* (1977), and Cygan (1991) for brines at 220K, respectively.

A basal He flux of 1.9×10^{-11} mol dm⁻² year⁻¹ (3.6×10^3 cm⁻² s⁻¹) is required to produce a surface He flux of 10^5 cm⁻² s⁻¹ for this diffusivity structure and the *in situ* He generation rates. This indicates that crustal degassing by diffusion alone produces a He flux that is comparable with

TABLE 2. MODEL PARAMETERS FOR THE MARTIAN CRUST

Species	Ice diffusivity (m ² year ⁻¹)	Supracryosphere diffusivity (m ² year ⁻¹)	In situ production rate (mol dm ⁻³ year ⁻¹)	Basal flux (mol dm ⁻² year ⁻¹)	Atmospheric partial pressure (atm)	Henry's constant (mol mol of H ₂ O ⁻¹ atm ⁻¹)	Atmospheric equilibrium concentration (mol dm ⁻³)
He	$10.7 e^{(-11,300/RT)}$	1×10^{11}	$1.5-4 \times 10^{-15}$	1.9×10^{-11}	6.6×10^{-8}	2.7×10^{-6}	7.9×10^{-9}
H ₂	$1.4 e^{(-750/RT)}$	1×10^{11}	$5.6-28 \times 10^{-12}$	0	2.0×10^{-6}	5.2×10^{-6}	5.7×10^{-7}
CH ₄	$2.5 e^{(-11,300/RT)}$	1×10^{11}	$1.4 \times 10^{-10} e^{(-0.00136z)a}$	1.9×10^{-10}	1.7×10^{-9}	6.5×10^{-5}	5.4×10^{-9}

^a*In situ* rate maximum sustainable by *in situ* H₂ production rate.

that estimated from earlier models (Krasnopolsky *et al.*, 1994; Krasnopolsky and Gladstone, 1996) and that volcanism is not a prerequisite for subsurface He flux. The subsurface abiogenic CH₄ flux corresponding to this basal He flux would be $\sim 1.9 \times 10^{-10} \text{ mol dm}^{-2} \text{ year}^{-1}$ ($3.6 \times 10^4 \text{ cm}^{-2} \text{ s}^{-1}$). The maximum microbial CH₄ surface flux was $\sim 1 \times 10^{-5} \text{ mol dm}^{-2} \text{ year}^{-1}$ ($2 \times 10^9 \text{ cm}^{-2} \text{ s}^{-1}$). The surface H₂ flux in the absence of microbial CH₄ consumption was $\sim 4 \times 10^{-6} \text{ mol dm}^{-2} \text{ year}^{-1}$ ($8 \times 10^8 \text{ cm}^{-2} \text{ s}^{-1}$). We note that this surface H₂ flux is $\sim 10\%$ of the $8.8 \times 10^9 \text{ cm}^{-2} \text{ s}^{-1}$ atmospheric production rate (Summers *et al.*, 2002) and, therefore, is not likely to significantly affect the $\delta^2\text{H}$ content of martian atmospheric H₂ even if it was not consumed at all. The model predicts a (H₂ + CH₄)/He surface flux ratio of $\sim 2,500$. This maximum *in situ* CH₄ production rate would only lead to a $\sim 1\%$ conversion of pore water into pore hydrate after a billion years. The model indicates that radiolytically produced H₂ suffices to support the observed CH₄ surface flux in the absence of any other H₂ sources. Most likely subsurface H₂ generated by other processes and atmospheric H₂ all contribute to the potential microbial CH₄ production rate.

The CH₄ flux depends upon the crustal model in the following ways. If a significant vadose zone exists between the base of the cryosphere (Clifford and Parker, 2001) and the water table, then the H₂ and CH₄ production rates will be significantly less because the H₂ radiolytic production rate in water vapor and the rate of microbial methanogenesis in unsaturated pore space will both be significantly reduced. The decrease in the total CH₄ production rate will be partly compensated by the higher diffusive transport rate across the vadose zone. At higher latitudes, where the surface temperatures are much lower and the base of the cryosphere extends to much greater depths, the H₂ production rates will remain the same, whereas CH₄ production rates will be substantially less than those at the equator.

This simple diffusive transport model for CH₄, H₂, and He to the martian surface has two caveats. First, because the CH₄ will combine with water ice to form hydrate under appropriate conditions of temperature and pressure, which on Mars is found at depths ranging from ~ 15 m below the surface to as much as a kilometer beneath the base of the cryosphere (Max and Clifford, 2000), it is unlikely to be able to diffuse through the cryosphere unless the potential storage ca-

capacity of the hydrate stability zone has been exceeded. This is not unreasonable because, regardless of whether the CH₄ is generated by biotic or abiotic processes, these processes have likely been active throughout Mars' geologic history. As the interior of the planet cooled, the freezing front at the base of the cryosphere propagated deeper into the crust at a rate of ~ 0.5 m Myr⁻¹ at the equator (Clifford and Parker, 2001). The models above predict that the sustainable rates of microbial CH₄ production would generate a subsurface flux of $\sim 10^9 \text{ cm}^{-2} \text{ s}^{-1}$. If all of this CH₄ were trapped as hydrate at the base of the cryosphere, then the hydrate propagation rate would be ~ 0.07 m Myr⁻¹. This suggests that the rate of cryosphere thickening has been more than sufficient to keep the hydrate stability zone from saturating. However, these simple models do not preclude the possibility that spatial or temporal spikes in the microbial methanogenesis rate could locally saturate the cryosphere with clathrates.

These arguments and model results suggest a means of distinguishing the four possible origins for the CH₄ that has been detected in the martian atmosphere: (1) volcanogenic; (2) sublimation of hydrate-rich ice; (3) diffusive transport through hydrate-saturated cryosphere; and (4) microbial CH₄ generation above the cryosphere. A volcanogenic source would generate ~ 20 times greater He surface flux as a result of the greater crustal degassing. The C₁–C₄ thermogenic compounds yield C and H isotopic profiles that distinguish them from abiogenic C₁–C₄ compounds (Sherwood Lollar *et al.*, 2002). To the extent that water on the martian surface is enriched in ²H, which is 5.2 times that of the Earth's, relative to the deep martian subsurface cryosphere or sub-cryosphere brine, the $\delta^2\text{H}$ of deeply sourced CH₄ might reflect the H isotopic composition of deeply seated, unenriched H₂O. Given the extent to which the H isotopic signature of hydrous phases of SNC meteorites records interaction with the enriched, near-surface H₂O inventory (Watson *et al.*, 1994), it remains uncertain as to whether the CH₄ of modern volcanism would do the same.

The second, and currently most plausible, origin is that the crustal emissions result from the sublimation of near-surface, hydrate-rich ice at low latitudes, where ground ice and hydrate are both thermodynamically unstable when they are in diffusive contact with the atmosphere. Theoretical calculations suggest that the resulting sub-

limation front, at latitudes between $\pm 30^\circ$, may have propagated down to depths ranging from just a few tens of centimeters to as much as a kilometer below the surface, depending on the local thermal and diffusive properties of the crust and the extent of replenishment from deeper H₂O reservoirs (Fanale *et al.*, 1986; Clifford, 1993; Mellon and Jakosky, 1993). For a sublimation rate of $\sim 3\text{--}6 \times 10^{-2} \text{ m Myr}^{-1}$ (Fanale *et al.*, 1986) at the equator and a cryosphere that is $\sim 14\%$ hydrate (from calculations above), the corresponding CH₄ surface flux would be $\sim 2\text{--}4 \times 10^7 \text{ cm}^{-2} \text{ s}^{-1}$. In this case, no correlation between CH₄ and He or H₂ surface flux would be observed, but a positive correlation between CH₄ and H₂O surface flux would be expected. Also, the $\delta^2\text{H}$ of the CH₄ should reflect the ²H-enriched H₂O of the martian surface.

If the cryosphere near the equator is effectively saturated with hydrate, then CH₄ may be originating from below the cryosphere and diffusing to the surface as modeled in this study. In this case the CH₄ and He surface flux would be correlated, but with higher (H₂ + CH₄)/He surface flux ratios than in the case of volcanogenic origin. The C and H isotopic profiles of the C₁–C₄ compounds, the C₁–C₄ relative abundances, and the CH₄/H₂ would all potentially distinguish microbial from abiogenic CH₄. The $\delta^2\text{H}$ of the CH₄ could reflect a mixture of CH₄ from the near-surface, ²H-enriched H₂O environment and deep-seated CH₄ from the unenriched H₂O environment.

The final potential origin is that the atmospheric CH₄ is produced in the shallow subsurface (Krasnopolsky *et al.*, 2004b), either above the hydrate stability zone (*i.e.*, $<15 \text{ m}$ depth) or above the local depth of the sublimation front, which, again, may lie as much as a kilometer beneath the surface at the equator. In this case, microbial CH₄ generation in a CaCl₂, or DEVIL, brine (Burt and Knauth, 2003) in a subsurface environment lying above the ice-saturated cryosphere might be sustained by a combination of radiolytic H₂ and atmospheric H₂. Brines may occur at such shallow depth if they are composed of salts like CaCl₂ and LiCl, which are capable of depressing the freezing point to 218K and below (Brass, 1980; Clark and Van Hart, 1981; Burt and Knauth, 2003). Any significant flux of CO₃²⁻ into this environment, however, would quickly strip calcium from the water and lead to freezing. This environment can only exist, therefore, if the pH is subneutral to

acidic or communication with the atmospheric CO₂ is limited. Given that low temperature, water–rock interactions lead to high pH because of hydrolysis of the silicates (Wallendahl and Treiman, 1999) the DEVIL brine environment would seem to require restricted access to the martian atmosphere. If the pore gas diffusivity for such an environment were $10^{11} \text{ m}^2 \text{ year}^{-1}$ ($0.32 \text{ cm}^2 \text{ s}^{-1}$), a value consistent with submicron pore throat sizes (Fanale *et al.*, 1986), and the environment were 100 m deep, then an *in situ* microbial CH₄ production rate of $\sim 6 \times 10^{-6} \text{ mol dm}^{-3} \text{ year}^{-1}$ would be required to generate the CH₄ surface flux of $1.8 \times 10^5 \text{ cm}^{-2} \text{ s}^{-1}$ (Krasnopolsky *et al.*, 1994). This *in situ* rate could not be sustained by the combined radiolytic and atmospheric H₂ fluxes and would require a 100 times greater H₂ flux. Terrestrial autotrophic methanogens, which utilize H₂ as their electron donor, however, are not known to exist in highly saline environments probably because of the energy demands of maintaining a proper osmotic gradient (Oren, 1999). In South Africa, methanogens are noticeably absent from the deep residing brines, which may in part explain the decline in the *in situ* microbial CH₄ rate more than any other factor. If martian methanogens are operating within DEVIL brine-saturated pores in the upper levels of the martian crust, then they may be metabolizing methylated C₁ compounds or dimethyl sulfide like their terrestrial counterparts (Oremland and King, 1989) or have evolved a more energy-efficient means of maintaining osmotic stability. In this scenario, CH₄ emissions may be correlated with local depletions in atmospheric H₂ or CO and, depending upon the depth of the environment, with martian season. They may also be correlated with suspected locations of brine seeps. The $\delta^2\text{H}$ of the CH₄ could reflect the depth of origin if the near-surface H₂O is significantly ²H enriched with respect to the deep-seated H₂O.

CH₄ DETECTION AND ANALYSIS ON MARS

The models in the preceding section suggest that measurements of the CH₄, He, and H₂ concentrations can yield valuable insights as to the origin of the CH₄ and whether it is a biomarker. Equally important is the determination of its C and H isotopic composition. To distinguish abio-

genic from microbial CH₄, measurement of the H and C isotopic composition of CH₄ and the abundance of higher hydrocarbons such as C₂H₆ offer the best approach. Although astronomical determinations of the isotopic composition of CH₄ may be feasible, they lack the precision necessary to partition the sources of CH₄ and will have to be corrected for significant isotopic fractionation produced by photochemical reactions that occur at altitudes greater than 120 km (Nair *et al.*, 2005). The most reliable and useful approach from an exploration perspective is to measure the CH₄ isotopic composition from orbit with an airborne vehicle like a Mars plane, or from a rover.

In terms of analytical approaches, cavity ring-down spectroscopy (CRDS) is a high-sensitivity infrared tunable laser spectrometer method for detection of the absorption spectra of trace gases (Busch and Busch, 1999). The gas sample to be studied is inserted into a stable optical cavity formed by two or more "super mirrors" with a reflectivity, R , that is greater than 99.99%. This optical cavity is excited either with a short pulse of light or with continuous wave light that is rapidly turned off from a narrow line width tunable laser. This leads to light being trapped inside the cavity, and this light intensity decays exponentially with time at a rate proportional to both the loss due to the mirrors and any absorption or scattering loss as the light propagates through the gas sample. The intra-cavity light intensity is monitored by the intensity of light being transmitted by one of the highly reflective mirrors. Without absorption, the average number of passes through the cell that a photon will make is $1/(1 - R)$, which can be between 10^4 and 10^5 with current state-of-the-art mirrors or a path length of ~ 3 – 30 km for a 30-cm-length cavity. Unlike traditional absorption methods, CRDS is completely independent of amplitude noise in the optical source since a change in the excitation power only affects the amplitude of the resulting exponential signal decay, but not its decay rate, which depends only on the gas sample's absorption coefficient after correction for the background loss rate.

The noise in the absorption coefficient that CRDS can measure is given by $(1 - R)/L$ (L being the distance between the mirrors, which for this illustration was chosen to be 30 cm) multiplied by the smallest fractional change in the ring-down decay rate that can be determined. The first factor can be as low as $5 \times 10^{-7} \text{ cm}^{-1}$, and the

second can be 7.7×10^{-4} or an overall noise-equivalent sensitivity of $\sim 4 \times 10^{-10}/\sqrt{n} \text{ cm}^{-1}$, where n is the number of ring-down events (Dudek *et al.*, 2003). For 1,000 ring-down events, equivalent to 0.07 s, the noise-equivalent sensitivity is $\sim 1 \times 10^{-11} \text{ cm}^{-1}$. This sensitivity is robust, both in controlled conditions and after transport and deployment in less ideal industrial settings (Yan *et al.*, 2001).

The possible use of CRDS to detect CH₄ in the martian atmosphere requires consideration of a number of factors. The strongest infrared absorption line of CH₄ is at 3067.3 cm⁻¹ with an integrated line strength of $2.13 \times 10^{-19} \text{ cm molecule}^{-1}$ at room temperature (Rothman *et al.*, 2005). This absorption line falls within the range of quantum cascade lasers (Yang *et al.*, 2005). If we assume the martian atmosphere to have a pressure of 4.6 Torr, a temperature of 213K, and a pressure broadening coefficient (half-width at half-maximum) of the CH₄ line by CO₂ of $0.085 \text{ cm}^{-1} \text{ atm}^{-1}$ (Walker and Philips, 1983), then the predicted CH₄ absorption cross section at the peak of the line is $1.3 \times 10^{-16} \text{ cm}^2$. The absorption coefficient, which determines the loss rate of the optical cavity in CRDS, is the product of the number density times the absorption cross section. Based upon the absorption sensitivity calculated above, we can predict a noise-equivalent CH₄ number density of $3.9 \times 10^5 \text{ cm}^{-3}$ (1σ in 0.07 s), which translates to a concentration of only 2 parts per trillion (pptv). This is only 2 parts in 10^4 of the martian CH₄ concentration reported by Krasnopolsky *et al.* (2004b). This demonstrates that a CRDS instrument, because of its sensitivity, can rapidly measure small changes in the CH₄ concentration with current technology. This compares favorably to an estimated detection limit of ~ 100 pptv for a hypothetical multipass Herriott cell with 40-m path length that integrates over eight absorption lines for ¹²CH₄ in the 3.3 μm spectral region for several minutes (Webster, 2005).

CRDS instruments have measured small changes in isotopic abundance of sample gases, such as CO₂, with a reported precision of $\delta^{13}\text{C}$ of 0.22‰ (Crosson *et al.*, 2002). A study of the isotopic composition of CH₄ in ambient air using a CRDS reported a precision for $\delta^{13}\text{C}$ of 11‰ for 10 2-s integrations, a precision that was limited by the poor signal-to-noise ratio of their CRDS instrument (the noise-equivalent sensitivity was $2 \times 10^{-9} \text{ cm}^{-1}$), which could have been improved by better acoustic isolation and more highly reflective mirrors (Dahnke *et al.*, 2001).

Both ¹³CH₄ (3057.97 cm⁻¹) and ¹²C²HH₃ (3005.11 cm⁻¹) have strong absorption lines in the same spectral region as ¹²CH₄, and these would be 1% and 0.06% as strong, assuming a CH₄ δ¹³C of -45‰ VPDB, with an abundance of 1.1237% for ¹³C, and a CH₄ δ²H of 2,252‰ Vienna Standard Mean Ocean Water (VSMOW), with an abundance of 0.01558% for ²H. This δ²H for CH₄ is equivalent to -350‰ relative to a martian hydrosphere that has 5.2 times the ²H abundance of the Earth's. This isotopic composition corresponds to a ¹³CH₄ concentration of 106 pptv and a ¹²C²HH₃ concentration of 12.6 pptv for a CH₄ concentration of 10 ppbv. If we assume the CH₄ detection limit of 2 pptv limits the accuracy of the isotopic ratio, then we could determine the δ¹³C with a 1σ of 23‰ and the δ²H with a 1σ of 876‰. These limits will scale inversely with CH₄ concentration so that for a martian CH₄ as high as 100 ppbv (Formisano *et al.*, 2004), the predicted precision would be 2.3‰ for δ¹³C and 88‰ for δ²H. At these levels of precision it is possible to resolve isotopically some of the different CH₄ reservoirs found in terrestrial samples (Fig. 1). To attain an analytical precision approaching the ±0.5‰ and ±5‰ for δ¹³C and δ²H for compound-specific isotope ratio mass spectrometers (Ward *et al.*, 2004), the 10 ppbv CH₄ of the martian atmosphere would have to be *preconcentrated* by a factor of ~47 and ~175 times, respectively. These levels of *preconcentration* are much less than the factors of 300 and 4,000 required by the theoretical 40-m path length multipass instrument described by Webster (2005), which achieves much poorer precision levels of ±10‰ and ±50‰ for δ¹³C and δ²H, respectively. In fact, Webster (2005) concluded that determination of the δ²H for martian atmospheric CH₄ by his theoretical multipass instrument is probably not feasible. The advantages of utilizing laser spectroscopy over mass spectrometry for martian rover missions have already been summarized by Webster (2005). This analysis demonstrates that isotopic variation of martian atmospheric CH₄ can be monitored with CRDS instruments that can be constructed with current technology and an accuracy approaching that of isotope ratio mass spectrometers.

To distinguish abiogenic CH₄ from thermogenic or biogenic sources, however, requires comparison of the δ¹³C of C₂H₆ with that of CH₄. Although the CH₄/C₂+ ratio of abiogenic hydrocarbons on Mars is difficult to predict, we can start by assuming that it would be similar to what

we see in the Precambrian Shield gases on Earth with CH₄/C₂+ of 10:1. The photochemical depletion of C₂H₆ with respect to CH₄ is ~25 (Krasnopolsky, 2005). If the source of the CH₄ were abiogenic, then concentration of 10 ppbv CH₄ would have corresponding C₂H₆ concentrations of 40 pptv, which is above the CRDS instrument's detection limit. *Preconcentration* of the C₂H₆ by a factor of ~1,000, however, would be required to achieve an isotopic determination of the δ¹³C of the C₂H₆ with sufficient accuracy (±5‰). The isotopic fractionation associated with such a drastic *preconcentration* would have to be evaluated carefully.

Although a single determination of the δ¹³C and δ²H of CH₄ alone will not necessarily determine whether it is biogenic or abiogenic, the variation of its isotopic composition with concentration over time may. The CRDS instrument when deployed on a rover will be able to record diurnal and seasonal changes and spatial variations in the concentration and isotopic composition of CH₄ in the martian atmosphere. A rover would use this information in conjunction with other data to identify CH₄ sources and sinks and whether either or both are biological in nature. Temporal variability that could be related to temperature changes in the near subsurface of Mars would be consistent with a potential biological source, especially if the isotopic composition varied dramatically given the magnitude of microbial isotopic discrimination. If microbial oxidation of CH₄ by reduction of O₂ (aerobic methanotrophy) or by reduction of sulfate to sulfide (anaerobic methanotrophy) was occurring, it would produce large isotopic fractionation shifts in the δ¹³C of the residual CH₄ (Coleman *et al.*, 1981; Alperin *et al.*, 1988; Reeburgh, 2003) that might distinguish it from the isotopic shifts in δ²H of CH₄ produced by abiotic oxidation of CH₄ caused by photochemical destruction (Nair *et al.*, 2005; see Fig. 1). On the martian surface at low latitudes where intermittent brine might occur as a result of diurnal temperature variation (Kuznetz and Gan, 2002), simple thermodynamic analysis of the aerobic methanotroph reaction yields a negative free energy of -750 kJ mol⁻¹, which is more than sufficient to sustain ATP production for terrestrial microorganisms. If methanotrophy is responsible for the CH₄ sink, then isotopic enrichment of the residual CH₄ will be substantial. Because the fractionation effects of photochemical destruction and microbial CH₄ ox-

idation are very similar based upon current data, the temporal observations of the martian CH₄ isotopic signature will be critical to resolving microbial from abiogenic signatures.

The final proof of microbial processes in the martian CH₄ cycle, however, requires direct detection of the cellular organic matter in a sample that exhibits a methanogenic or methanotrophic metabolism. For this reason, the principal importance of the CRDS would be to analyze spatial variations in concentration of atmospheric CH₄ and changes correlated with shifts in the wind direction that, in turn, could be utilized to steer the rover toward the source (or sink). The CRDS instrument could also be utilized for analyses of solid phases, *e.g.*, CH₄ hydrate, with an appropriate degassing/volatilization compartment, thus acting as a metabolic-based life detection tool. It is anticipated that, with minor modification, the instrument could be used to detect other molecular species present at low concentrations, most particularly other small hydrocarbons such as ethylene and ethane.

Given that a flight-capable CRDS instrument will not be available for the instrument packages already proposed for the Mars Surface Laboratory, the Astrobiology Field Laboratory is the next logical target for implementation of CRDS. This hypothetical post-Mars Surface Laboratory rover mission to Mars is named in various Mars Exploration Program Advisory Group pathways and could precede, parallel, or even follow a Mars Sample Return program. The Astrobiology Field Laboratory option essentially presumes that martian habitability, indeed past or present life itself on Mars, remains a real possibility warranting additional focused *in situ* study with a rover. The first possible launch opportunity considered is in 2013. The isotopic signature of CH₄ represents one biosignature for which a virtually limitless number of samples can be analyzed. Even though the CH₄ source or sinks may be beyond the reach of the Astrobiology Field Laboratory (*e.g.*, >1 m deep), it is conceivable that access to the subsurface via crater cuts or erosion channels may provide solid samples of the environmental niches that once supported ancient methanogenesis or methanotrophy.

Since the CRDS instrument measures air samples through a filter and does not come into direct contact with Mars surface samples, its degree of internal organic cleanliness and sterility does not have to match that of contact instruments. It

will be extremely important, however, for the *pre-concentrator* and sample/cavity interface to be free of any contaminating terrestrial methanogens and methanotrophs in the unlikely event that they become metabolically active on Mars and alter the CH₄ concentration and isotopic signature.

With regard to future deep-drilling missions on Mars (10–100 m), the CRDS instrument could provide real-time analyses of gases released from boreholes during drilling and aid in identifying rock layers that may require more detailed analyses of core samples or drill cuttings.

CONCLUSIONS

Extrapolation of the South African He, H₂, and CH₄ cycle to the martian subsurface indicates that the H₂ generation by radiolysis of ice and water can produce in reaction with CO₂ sufficient CH₄ to account for the recent observations of martian CH₄. The estimated *in situ* rate of H₂ production by radiolysis is sufficient to support a CH₄ surface flux of $\sim 10^9$ cm⁻² s⁻¹, given a modeled martian He surface flux of $\sim 10^5$ cm⁻² s⁻¹. Because of the colder environment, the predicted (CH₄ + H₂)/He flux rates would be significantly greater than that observed in South Africa, and this parameter may provide a means of distinguishing hot, volcanogenic CH₄ sources from cold, cryospheric sources. Abiogenic CH₄ originating from deep beneath the cryosphere might be distinguishable from microbial CH₄ by determining its C and H isotopic composition relative to that of C₂H₆. If CH₄ hydrate exists within the cryosphere, then the CH₄ surface flux may be related to sublimation from the top of the cryosphere, in which case CH₄ atmospheric gas concentrations should be correlated to atmospheric H₂O. Microbial CH₄ generated in near-surface hypersaline environments above the hydrate stability zone could contribute to the CH₄ surface flux, but only if a much greater electron donor flux is being tapped, in which case the CH₄ atmospheric gas concentrations may be negatively correlated with atmospheric H₂ and CO. If the martian hydrosphere is isotopically zoned with ²H-enriched H₂O located at the surface and ²H-depleted H₂O located at depth, then the $\delta^{2\text{H}}$ of the CH₄ may reflect the depth of origin of the CH₄. Diurnal and seasonal variations in the CH₄ abundance and isotopic composition would also constrain its ori-

gin and pinpoint the source of the emissions. A flight-capable version of a CRDS apparatus represents the type of instrument that has the sensitivity required to perform such an analyses. Such an instrument could be utilized to guide a rover to the location of CH₄ emissions or consumptions to perform life detection experiments.

ACKNOWLEDGMENTS

This research was supported by NASA Astrobiology Institute grant to Prof. L.M. Pratt of Indiana University. The manuscript benefited immensely from assiduous reviews by Vladimir Krasnopolsky and Norm Sleep.

ABBREVIATIONS

C₂+, ethane + propane + butane; CRDS, cavity ring-down spectroscopy; Ga, × 10⁹ year old; Myr, 10⁶ years; ppbv, parts per billion; ppmv, parts per million; pptv, parts per trillion; VDPB, Vienna Pee Dee Formation Belemnite standard; VSMOW, Vienna Standard Mean Ocean Water.

REFERENCES

- Abrajano, T.A., Sturchio, N.C., Bohlke, J.K., Lyon, G.L., Poreda, R.J., and Stevens, C.M. (1988) Methane-hydrogen gas seeps, Zambales Ophiolite, Philippines: deep or shallow origin. *Chem. Geol.* 71, 211–222.
- Abrajano, T.A., Sturchio, N.C., Kennedy, B.M., Lyon, G.L., Muehlenbachs, K., and Bohlke, K.J. (1990) Geochemistry of reduced gases related to serpentinization of the Zambales ophiolite, Philippines. *Appl. Geochem.* 5, 625–630.
- Alperin, M.J., Reeburgh, W.S., and Whiticar, M.J. (1988) Carbon and hydrogen isotope fractionation resulting from anaerobic methane oxidation. *Global Biogeochem. Cycles* 2, 279–288.
- Andrews, J.N., Hussain, N., and Youngman, M.J. (1989) Atmospheric and radiogenic gases in groundwaters from the Stripa granite. *Geochim. Cosmochim. Acta* 53, 1831–1841.
- Brass, G.W. (1980) Stability of brines on Mars. *Icarus* 42, 20–28.
- Burt, D.M. and Knauth, L.P. (2003) Electrically conducting, Ca-rich brines, rather than water, expected in the Martian subsurface. *J. Geophys. Res.* 108, 8026, doi:10.1029/2002JE001862.
- Busch, K.W. and Busch, M.A. (1999) Cavity-ringdown spectroscopy: an ultrasensitive-absorption measurement technique. *ACS Symp. Ser.* 720, 269.
- Chen, J.H. and Wasserburg, G.J. (1985) Formation ages and evolution of Shergotty and its parent planet from U-Th-Pb systematics. *Geochim. Cosmochim. Acta* 50, 955–968.
- Clark, B.C. and Van Hart, D.C. (1981) The salts of Mars. *Icarus* 45, 370–378.
- Clifford, S.M. (1993) A model for the hydrologic and climatic behavior of water on Mars. *J. Geophys. Res.* 98, 10973–11016.
- Clifford, S.M. and Parker, T.J. (2001) The evolution of the martian hydrosphere: implications for the fate of a primordial ocean and the current state of the Northern Plains. *Icarus* 154, 40–79.
- Coleman, D.D., Risatti, J.B., and Schoell, M. (1981) Fractionation of carbon and hydrogen isotopes by methane-oxidizing bacteria. *Geochim. Cosmochim. Acta* 45, 1033–1037.
- Crosson, E.R., Ricci, K.N., Richman, B.A., Chilese, F.C., Owano, T.G., Povencal, R.A., Todd, M.W., Glasser, J., Kachanov, A.A., Paldus, B.A., Spence, T.G., and Zare, R.N. (2002) Stable isotope ratios using cavity ring-down spectroscopy: determination of ¹³C/¹²C for carbon dioxide in human breath. *Anal. Chem.* 74, 2003–2007.
- Cussler, E.L. (1985) *Diffusion: Mass Transfer in Fluid Systems*, Cambridge University Press, Cambridge, p. 525.
- Cygan, R.T. (1991) *The Solubility of Gases in NaCl Brine and a Critical Evaluation of Available Data*, Sandia Report SAND90-2848 UC-721, DOE Sandia National Laboratory, Albuquerque, NM, p. 98.
- Dahnke, H., Kleine, D., Urban, W., Hering, P., and Murtz, M. (2001) Isotopic ratio measurement of methane in ambient air using mid-infrared lead-out spectroscopy. *Appl. Phys. B* 72, 121–125.
- Des Marais, D.J., Donchin, J.H., Nehring, N.L., and Truesdell, A.H. (1981) Molecular carbon isotopic evidence for the origin of geothermal hydrocarbons. *Nature* 292, 826–828.
- Dudek, J.B., Tarsa, P.B., Velasquez, A., Wladyslawski, M., Rabinowitz, P., and Lehmann, K.K. (2003) Trace moisture detection using continuous-wave cavity ring-down spectroscopy. *Anal. Chem.* 75, 4599–4609.
- Fanale, F.P., Salvail, J.R., Zent, A.P., and Postawko, S.E. (1986) Global distribution and migration of subsurface ice on Mars. *Icarus* 67, 1–18.
- Formisano, V., Atreya, S., Encrenaz, T., Ignatiev, N., and Giuranna, M. (2004) Detection of methane in the atmosphere of Mars. *Science* 306, 1758–1761.
- Fritz, P., Clark, I.D., Fontes, J.-C., Whiticar, M.J., and Faber, E. (1992) Deuterium and ¹³C evidence for low temperature production of hydrogen and methane in a highly alkaline groundwater environment in Oman. In *Water-Rock Interaction*, edited by H. Kharaka and A. Maest, Balkema, Rotterdam, pp. 793–796.
- Gordon, L.I., Cohen, Y., and Standley, D.R. (1977) The solubility of molecular hydrogen in seawater. *Deep-Sea Res.* 24, 937–941.
- Hoehler, T.M., Alperin, M.J., Albert, D.B., and Martens, C.S. (1998) Thermodynamic control on hydrogen concentrations in anoxic sediments. *Geochim. Cosmochim. Acta* 62, 1745–1756.

- Horita, J. and Berndt, M.E. (1999) Abiogenic methane formation and isotopic fractionation under hydrothermal conditions. *Science* 285, 1055–1057.
- Hunt, J.M. (1996) *Petroleum Geochemistry and Geology*, W.H. Freeman, New York, p. 743.
- Ikeda-Fukazawa, T., Horikawa, S., Hondoh, T., and Kawamura, K. (2002) Molecular dynamics studies of molecular diffusion ice Ih. *J. Chem. Phys.* 117, 3886–3896.
- Kelley, D.S., Karson, J.A., Fruh-Green, G.L., Yoerger, D.R., Shank, T.M., Butterfield, D.A., Hayes, J.M., Schrenk, M.O., Olson, E.J., Proskurowski, G., Jakuba, M., Bradley, A., Larson, B., Ludwig, K., Glickson, D., Buckman, K., Bradley, A.S., Brazelton, W.J., Roe, K., Elend, M.J., Delacour, A., Bernasconi, S.M., Lilley, M.D., Baross, J.A., Summons, R.E., and Sylva, S.P. (2005) A serpentinite-hosted ecosystem: the Lost City Hydrothermal Field. *Science* 307, 1428–1434.
- Krasnopolsky, V.A. (2005) Some problems related to the origin of methane on Mars. *Icarus* 180, 359–367.
- Krasnopolsky, V.A. and Gladstone, G.R. (1996) Helium on Mars: EUVE and PHOBOS data and implications for Mars' evolution. *J. Geophys. Res.* 101, 15765–15772.
- Krasnopolsky, V.A. and Gladstone, G.R. (2005) A sensitive search for SO₂ in the martian atmosphere: implications for seepage and origin of methane. *Icarus* 178, 487–492.
- Krasnopolsky, V.A., Bowyer, S., Chakrabarti, S., Gladstone, G.R., and McDonald, J.S. (1994) First measurement of helium on Mars: implications for the problem of radiogenic gases on the terrestrial planets. *Icarus* 109, 337–351.
- Krasnopolsky, V.A., Maillard, J.P., and Owen, T.C. (2004a) Detection of methane in the martian atmosphere: evidence for life [abstract 06169]. In *Geophysical Research Abstracts* 6, EGU Congress, Katlenburg-Lindau, Germany.
- Krasnopolsky, V.A., Maillard, J.P., and Owen, T.C. (2004b) Detection of methane in the martian atmosphere: evidence for life? *Icarus* 172, 537–547.
- Kress, M.E. and McKay, C.P. (2004) Formation of methane in comet impacts: implications for Earth, Mars, and Titan. *Icarus* 168, 475–483.
- Kuznetz, L.H. and Gan, D.C. (2002) On the existence and stability of liquid water on the surface of Mars today. *Astrobiology* 2, 183–195.
- Lin, L.-H., Slater, G.F., Sherwood Lollar, B., Lacrampe-Couloume, G., and Onstott, T.C. (2005a) The yield and isotopic composition of radiolytic H₂, a potential energy source for the deep subsurface biosphere. *Geochim. Cosmochim. Acta* 69, 893–903.
- Lin, L.-H., Hall, J.A., Lippmann, J., Ward, J.A., Sherwood Lollar, B., and Onstott, T.C. (2005b) Radiolytic H₂ in the continental crust: nuclear power for deep subsurface microbial communities. *Geochim. Geophys. Geosyst.* 6, 10.1029/2004GC000907.
- Lippmann, J., Stute, M., Torgersen, T., Moser, D.P., Hall, J., Lin, L., Borcsik, M., Bellamy, R.E.S., and Onstott, T.C. (2003) Dating ultra-deep mine waters with noble gases and ³⁶Cl, Witwatersrand Basin, South Africa. *Geochim. Cosmochim. Acta* 67, 4597–4619.
- Lyons, J.R., Manning, C.E., and Nimmo, F. (2005) Formation of methane on Mars by fluid-rock interaction in the crust. *Geophys. Res. Lett.* 32, doi:10.1029/2004GL022161. L13201.
- Max, M.D. and Clifford, S.M. (2000) The state, potential distribution and biological implications of methane in the martian crust. *J. Geophys. Res.* 105, 4165–4171.
- Mellon, M.T. and Jakosky, B.M. (1993) Geographic variations in the thermal and diffusive stability of ground ice on Mars. *J. Geophys. Res.* 98, 3345–3364.
- Mumma, M.J., Novak, R.E., DiSanti, M.A., Bonev, B.P., and Dello Russo, N. (2004) Detection and mapping of methane and water on Mars [abstract 26.02]. In *DPS Meeting 36*, American Astronomical Society, Washington, DC.
- Nair, H., Summers, M.E., Miller, C.E., and Yung, Y.L. (2005) Isotopic fractionation of methane in the martian atmosphere. *Icarus* 175, 32–35.
- Omar, G., Onstott, T.C., and Hoek, J. (2003) The origin of deep subsurface microbial communities in the Witwatersrand Basin, South Africa as deduced from apatite fission track analyses. *Geofluids* 3, 69–80.
- Onstott, T.C., Lin, L.-H., Davidson, M., Mislowack, B., Borcsik, M., Hall, J., Slater, G.F., Ward, J., Sherwood Lollar, B., Lippmann-Pipke, J., Boice, E., Pratt, L.M., Pfiffner, S.M., Moser, D.P., Gihring, T., Kieft, T.L., Phelps, T.J., van Heerden, E., Litthaur, D., DeFlaun, M., and Rothmel, R. (2005) The origin and age of biogeochemical trends in deep fracture water of the Witwatersrand Basin, South Africa. *Geomicrobiol. J.* (in press).
- Oremland, R.S. and King, G.M. (1989) Methanogenesis in hypersaline environments. In *Microbial Mats Physiological Ecology of Benthic Microbial Communities*, edited by Y. Cohen and E. Rosenberg, American Society for Microbiology, Washington, DC, pp. 180–190.
- Oren, A. (1999) Bioenergetic aspects of halophilism. *Microbiol. Mol. Biol. Rev.* 63, 334–348.
- Owen, T.C. (1992) Composition and early history of the atmosphere. In *Mars*, edited by H.H. Kieffer, B.M. Jakowski, C.W. Snyder, and M.S. Matthews, University of Arizona Press, Tucson, pp. 818–834.
- Oze, C. and Sharma, M. (2005) Have olivine, will gas: serpentinization and the abiogenic production of methane on Mars. *Geophys. Res. Lett.* 32, L10203.
- Price, P.B. and Sowers, T. (2004) Temperature dependence of metabolic rates for microbial growth, maintenance, and survival. *Proc. Natl. Acad. Sci. USA* 101, 4631–4646.
- Reeburgh, W.S. (2003) Global methane biogeochemistry. In *Treatise on Geochemistry, Vol. 4*, edited by R.J. Keeling, Elsevier Ltd., London, pp. 65–89.
- Rieder, R., Gellert, R., Anderson, R.C., Bruckner, J., Clark, B.C., Dreibus, G., Economou, T., Klingelhofer, G., Lugmair, G.W., Ming, D.W., Squyres, S.W., d'Uston, C., Wanke, H., Yen, A., and Zipfel, J. (2004) Chemistry of rocks and soils at Meridiani Planum from the Alpha Particle X-ray Spectrometer. *Science* 306, 1746–1749.
- Rothman, L.S., Jacquemart, D., Barbe, A., Benner, D.C., Birk, M., Brown, L.R., Carleer, M.R., Chackerian, C., Chance, K., Coudert, L.H., Dana, V., Devi, V.M., Flaud, J.M., Gamache, R.R., Goldman, A., Hartmann, J.M.,

- Jucks, K.W., Maki, A.G., Mandin, J.Y., Massie, S.T., Orphal, J., Perrin, A., Rinsland, C.P., Smith, M.A.H., Tennyson, J., Tolchenov, R.N., Toth, R.A., Vander Auwera, J., Varanasi, P., and Wagner, G. (2005) The HITRAN 2004 molecular spectroscopic database. *J. Quant. Spectrosc. Radiat. Transfer* 96, 139–204.
- Schoell, M. (1988) Multiple origins of methane in the Earth. *Chem. Geol.* 71, 1–10.
- Seyfried, W.E., Jr. and Mottl, M.J. (1995) Geologic setting and chemistry of deep-sea hydrothermal vents. In *The Microbiology of Deep-Sea Hydrothermal Vents*, edited by D.M. Karl, CRC Press, Boca Raton, FL, pp. 1–34.
- Sherwood Lollar, B., Frape, S.K., Weise, S.M., Fritz, P., Macko, S.A., and Welhan, J.A. (1993a) Abiogenic methanogenesis in crystalline rocks. *Geochim. Cosmochim. Acta* 57, 5087–5097.
- Sherwood Lollar, B., Frape, S.K., Fritz, P., Macko, S.A., Welhan, J.A., Blomqvist, R., and Lahermo, P.W. (1993b) Evidence for bacterially generated hydrocarbon gas in Canadian Shield and Fennoscandian Shield rocks. *Geochim. Cosmochim. Acta* 57, 5073–5085.
- Sherwood Lollar, B., Westgate, T.D., Ward, J.A., Slater, G.F., and Lacrampe-Couloume, G. (2002) Abiogenic formation of alkanes in the Earth's crust as a minor source for global hydrocarbon reservoirs. *Nature* 416, 522–524.
- Sherwood Lollar, B., Lacrampe-Couloume, G., Slater, G.F., Ward, J., Moser, D.P., Gihring, T.M., Lin, L.-H., and Onstott, T.C. (2005) Unravelling abiogenic and biogenic sources of methane in the Earth's deep subsurface. *Chem. Geol.* 226, 328–339.
- Shink, B. (1997) Energetics of syntrophic cooperation in methanogenic degradation. *Microbiol. Mol. Biol. Rev.* 61, 262–280.
- Shuster, D.L., Farley, K.A., Sisterson, J.M., and Burnett, D.S. (2004) Quantifying the diffusion kinetics and spatial distributions of radiogenic ⁴He in minerals containing proton-induced ³He. *Earth Planet. Sci. Lett.* 217, 19–32.
- Smith, S.P. and Kennedy, B.M. (1983) The solubility of noble gases in water and NaCl brine. *Geochim. Cosmochim. Acta* 47, 503–515.
- Spinks, J.W.T. and Woods, R.J. (1990) *An Introduction to Radiation Chemistry*, Wiley, New York, p. 574.
- Stevens, T.O. and McKinley, J.P. (1995) Lithoautotrophic microbial ecosystems in deep basalt aquifers. *Science* 270, 450–454.
- Strauss, H.L., Chen, Z., and Loong, C.-K. (1994) The diffusion of H₂ in hexagonal ice at low temperatures. *J. Chem. Phys.* 101, 7177–7180.
- Summers, M.E., Lieb, B.J., Chapman, E., and Yung, Y.L. (2002) Atmospheric biomarkers of subsurface life on Mars. *Geophys. Res. Lett.* 29, 2171–2174.
- Walker, H.C., Jr. and Philips, W.J. (1983) The collisional half width for the R(0) line of the 3 band of methane. *J. Appl. Phys.* 54, 4729–4733.
- Wallendahl, A. and Treiman, A.H. (1999) Geochemical models of low-temperature alteration of martian rocks [abstract 1268]. In *30th Lunar and Planetary Science Conference Abstracts*, LPI Contribution No. 964, Lunar and Planetary Institute, Houston.
- Ward, J.A., Slater, G.F., Moser, D.P., Lin, L.-H., Lacrampe-Couloume, G., Bonin, A.P., Davidson, M., Hall, J.A., Mislowack, B., Bellamy, R.E.S., Onstott, T.C., and Sherwood Lollar, B. (2004) Microbial hydrocarbon gases in the Witwatersrand Basin, South Africa: implications for the deep biosphere. *Geochim. Cosmochim. Acta* 68, 3239–3250.
- Watson, L.L., Hutcheon, I.D., Epstein, S., and Stolper, E.M. (1994) Water on Mars: clues from deuterium/hydrogen and water contents of hydrous phases in SNC meteorites. *Science* 265, 86–90.
- Webster, C.R. (2005) Measuring methane and its isotopes ¹²CH₄, ¹³CH₄, and CH₃D on the surface of Mars with *in situ* laser spectroscopy. *Appl. Optics* 44, 1226–1235.
- Welhan, J.A. and Craig, H. (1979) Methane and hydrogen in East Pacific Rise hydrothermal fluids. *Geol. Res. Lett.* 6, 829–831.
- Welhan, J.A., Faber, E., and Schoell, M. (1979) Gas chemistry and helium isotopes at Cerro Prieto. *Geothermics* 8, 241–244.
- Wong, A.-S. and Atreya, S.K. (2003) Chemical markers of possible hot spots on Mars. *J. Geophys. Res.* 108, 7-1–7-11.
- Yan, W.-B., Dudek, J.B., Lehmann, K.K., and Rabinowitz, P. (2001) A fast innovative infrared analyzer for monitoring ultra-trace moisture in semiconductor gases. In *Technical Paper 416*, Instrumentation, Systems, and Automation Society, Research Triangle Park, NC, pp. 247–256.
- Yang, R.Q., Hill, C.J., and Yang, B.H. (2005) High temperature and low threshold midinfrared interband cascade laser. *Appl. Phys. Lett.* 87, 151109–151111.
- Yuen, G., Blair, N., DesMarais, D.J., and Chang, S. (1984) Carbon isotope composition of low molecular weight hydrocarbons and monocarboxylic acids from Murchison meteorite. *Nature* 307, 252–254.

Address reprint requests to:

T.C. Onstott

Department of Geosciences

Princeton University

Princeton, NJ 08544

E-mail: tullis@princeton.edu